

# Effects of particle-hole fluctuations on the superfluid transition in two-dimensional atomic Fermi gases

Junru Wu,<sup>1,2,3</sup> Zongpu Wang,<sup>1,4</sup> Lin Sun,<sup>3,2</sup> Kaichao Zhang,<sup>1,2,3</sup> Chuping Li,<sup>1,2,3</sup>  
Yuxuan Wu,<sup>1,2,3</sup> Pengyi Chen,<sup>1,2,3</sup> Dingli Yuan,<sup>1,2,3</sup> and Qijin Chen<sup>1,2,3,\*</sup>

<sup>1</sup>Hefei National Research Center for Physical Sciences at the Microscale and School of Physical Sciences,  
University of Science and Technology of China, Hefei, Anhui 230026, China

<sup>2</sup>Shanghai Research Center for Quantum Science and CAS Center for Excellence in Quantum Information and Quantum Physics,  
University of Science and Technology of China, Shanghai 201315, China

<sup>3</sup>Hefei National Laboratory, University of Science and Technology of China, Hefei 230088, China

<sup>4</sup>Department of Physics, University of Hong Kong, Pokfulam Road, Hong Kong

(Dated: March 13, 2026)

Proper treatment of the many-body interactions is of paramount importance in our understanding of strongly correlated systems. Here we investigate the effects of particle-hole fluctuations on the Berezinskii-Kosterlitz-Thouless (BKT) transition in two-dimensional Fermi gases throughout the entire BCS-BEC crossover. We include self-consistently in the self energy treatment the entire particle-hole  $T$  matrix, which constitutes a renormalization of the bare interaction that appears in the particle-particle scattering  $T$  matrix, leading to a screening of the pairing interaction and hence a reduction of the pairing gap and the transition temperature  $T_{\text{BKT}}$ . Here  $T_{\text{BKT}}$  is determined by the critical phase space density, for which the pair density and pair mass are determined using a pairing fluctuation theory, which accommodates self-consistently the important self-energy feedback in the treatment of finite-momentum pairing fluctuations. The screening strength varies continuously from its maximum in the BCS limit to essentially zero in BEC limit. In the unitary regime, it leads to an interaction-dependent shift of  $T_{\text{BKT}}$  towards the BEC regime. This shift is crucial in explaining experimental data, when quantitiveness is important, as they often depend on the interaction strength. Where experimental and simulation data are available, our findings are consistent with experiment in the unitary and BEC regimes and with quantum Monte Carlo simulations in the BCS and unitary regimes.

## I. INTRODUCTION

Strongly correlated systems constitute a main challenge and are thus at the heart and frontier of condensed matter physics. Due to the low dimensionality, fluctuations in two dimensions (2D) are usually strong, positioning the system in the strongly correlated regime, for which a proper treatment of interaction effects is of paramount importance, in order to understand various experiments and physical phenomena at a *quantitative* level.

In the absence of long range order à la the Mermin-Wagner theorem [1], phase transition in 2D is in general of the Berezinskii [2], Kosterlitz and Thouless (BKT) [3] type. Indeed, superfluid transitions in ultracold atomic Bose gases have been experimentally found to exhibit a strong BKT nature in 2D [4–6]. BKT transitions have been of wide interest since the most important high  $T_c$  superconductors are quasi-2D layered materials [7], for which the low dimensionality is favorable for the formation of the wide-spread pseudogap phenomena, which are arguably attributable to strong fluctuations [8, 9]. It is also the model commonly used for describing the superconducting transition in thin films [10, 11]. Recent exciting discoveries of (quasi-)2D superconductors [12–15] have added to the interest in 2D phase transitions. The BKT nature of the superfluid transition in 2D atomic Fermi gases has also been experimentally confirmed [16, 17]. There are also, albeit not many, theoretical studies of the BKT superfluid transition

in a 2D Fermi system for both weak and strong pairing interactions, e.g., Ref. [18, 19].

In this paper, we report our study on the important yet often neglected effect of the particle-hole fluctuations on 2D Fermi gas superfluidity throughout the BCS-BEC crossover, to which similar studies has not been reported in the literature [19]. Similar to its 3D counterpart, we find that particle-hole fluctuations lead to a screening to the pairing interaction, causing a shift of the superfluid transition curve toward the BEC regime as a function of the pairing strength. This substantially suppresses  $T_c$  and the gap in the BCS and unitary regimes, and has an important physical significance when comparing between theory and experiment.

It is important to note that there has been a historical controversy surrounding 2D fermionic superfluids, dating back to Kosterlitz and Thouless [3], which primarily concerns observable signatures and the applicability of BKT physics. It is not straightforward to apply the BKT theory based on the XY model to fermionic superfluids. In the XY model, in which the superfluid density  $n_s/m$  provides the phase stiffness, it is the phase fluctuations of the vortex type that dominate the destruction of the quasi-long range superfluid order and drive the system into a disordered normal state. Unlike the superfluids of true bosons, however, the superfluid density is also suppressed by the pair-breaking Bogoliubov quasiparticle excitations as the temperature  $T$  increases. In addition, both the density and the mass of the bosons (i.e., fermion pair) now depend on the temperature and the pairing interaction strength, except in the deep BEC regime. Therefore, computing the superfluid density using a mean-field approximation would yield a constant value  $n_s/m = n/m$  at  $T = 0$  (or  $n/4m$  from the

\* Corresponding author: qjc@ustc.edu.cn

boson point of view, with  $n_B = n/2$  and  $M_B = 2m$ ), independent of the interaction strength. (Following standard notations, here  $n$ ,  $m$ ,  $n_B$ ,  $M_B$  and  $n_s$  denote total fermion number density, fermion mass, Cooper pair number density, Cooper pair mass, and superfluid number density, respectively.) At finite  $T$ , the pair-breaking effect due to quasiparticle excitations can be partly accounted for via solving the mean-field BCS gap equation, leading to a mean-field result of  $(n_s/m)^{\text{BCS}}$ . However, not being able to properly take care of the effective pair mass and pair number density is thus expected to give rise to an overestimate of the superfluid transition temperature  $T_{\text{BKT}}$ . Indeed, the fact  $T_{\text{BKT}}$ , as measured experimentally in 2D atomic Fermi gases, varies with interaction strength, reflects that both  $n_B$  and  $M_B$  vary with the interaction.

The pair number density at given temperature and interaction is normally governed by the pair dispersion. The latter, or equivalently pair mass, can, in principle, be extracted from the pair propagator. However, there are not many calculations of the fermionic  $T_{\text{BKT}}$  in the literature [20–23], partly due to the inapplicability of the simple XY model directly to the Fermi system. The fact that  $(n_s/m)^{\text{BCS}}$  decreases with temperature below  $T_{\text{BKT}}$  in the BCS regime manifests that amplitude fluctuations play an important role. Therefore, the superfluid transition in a 2D Fermi gas has a much richer physics than the simple XY model can capture. To account for the finite temperature and interaction effects, Wu et al [24] and Wang et al Ref. [18] determined  $T_{\text{BKT}}$  using the critical phase space density criterion, based on a quantum Monte Carlo simulation [25] along with experimental support [17]. A pairing fluctuation theory [26] that was developed to address the pseudogap phenomena in 3D superconductors was used to determine the effective pair number density  $n_B$  and pair mass  $M_B$ , which reflect the effects of both amplitude and phase fluctuations, governed by temperature and interaction strength. Nevertheless, these earlier works [18, 26] considered only the particle-particle channel of the  $T$ -matrix.

It has been known that particle-hole fluctuations may play an important role in the 3D superfluid behavior, despite that they are often neglected in theoretical treatments of superconductivity [27]. Gor'kov and Melik-Barkhudarov (GMB) [28] first found that the lowest order particle-hole fluctuations may reduce both  $T_c$  and the zero temperature gap  $\Delta_0$  by a factor of 0.44 in a BCS superconductor. The study of the GMB effect at the lowest order were extended to atomic Fermi gases in the continuum [29] or an optical lattice [30]. The effect beyond the lowest order, by including the full particle-hole  $T$ -matrix in a ladder approximation has been studied without [31] and with [32] the self-energy feedback.

In 2D, there have been no similar studies in the context of BCS-BEC crossover in the literature, however, except for the lowest order particle-hole contributions in the BCS limit [33]. It is the purpose of the present work to investigate the effect of particle-hole fluctuations on the Fermi gas superfluidity in 2D. The low dimensionality further enhances the strong pairing fluctuations, which are already present when the interaction is strong. The very BKT nature of the transition requires that there is already a sizable pairing amplitude, i.e., (pseudo)gap, at  $T_{\text{BKT}}$ . Therefore, this necessitates the self-

consistent inclusion of the self-energy feedback in (both the particle-particle and) the particle-hole  $T$ -matrices. Here we incorporate the particle-hole channel contributions in the pairing fluctuation theory [26, 32, 34], and thus go beyond previous studies [18, 24]. This pairing fluctuation theory includes self-consistently the finite-momentum pairing fluctuations in the single-fermion self energy, and has successfully addressed multiple high  $T_c$  [26, 34–36] and atomic Fermi gas experiments [37–40]. In particular, it features naturally a pseudogap in 3D unitary Fermi gases, which has been unequivocally corroborated by a recent experiment [41]. Following the previous work in 3D [32], we show that the particle-hole  $T$ -matrix serves as a renormalized pairing interaction, which is to appear in the  $T$ -matrix in the usual particle-particle channel. We find that the particle-hole fluctuations lead to a screening to the pairing interaction, and the inverse pairing interaction is effectively shifted by the temperature-dependent, angular-averaged (at two different levels) particle-hole susceptibility  $\langle\chi_{\text{ph}}\rangle$ , which approaches a negative constant,  $-m/2\pi$ , in the BCS limit and increases gradually in the crossover regime toward zero in the BEC limit. In result, the particle-hole channel shifts the  $T_{\text{BKT}}$  curve towards the BEC regime as a function of pairing strength. Furthermore, comparison shows that the inclusion of particle-hole channel leads to a better overall agreement between our calculated  $T_{\text{BKT}}$  with the results from experiment and quantum Monte Carlo simulations.

## II. THEORETICAL FORMALISM

### A. Overview of the Pair Fluctuation Theory without the Particle-Hole Channel

To be self-contained, we first recapitulate the pairing fluctuation theory [24, 26, 34] without including the particle-hole channel. This serves as a basis, on top of which the particle-hole channel effect is built. Note that here we will consider only the formalism without the superfluid order parameter, tailored for 2D in the absence of a true long range order.

We consider a 2D Fermi gas with a short-range  $s$ -wave attractive interaction  $V_{\mathbf{k},\mathbf{k}'} = U < 0$ , as described by a generic grand canonical Hamiltonian [34], which includes pairing with a finite center-of-mass momentum  $\mathbf{q}$ . The free fermion dispersion is given by  $\xi_{\mathbf{k}} = \epsilon_{\mathbf{k}} - \mu \equiv \mathbf{k}^2/2m - \mu$ , with chemical potential  $\mu$ . The Fermi momentum is  $\hbar k_F = \sqrt{2\pi n \hbar}$ , and Fermi energy  $E_F \equiv k_B T_F = \hbar^2 k_F^2/2m$ . As usual, we shall use the natural units, and set  $\hbar = k_B = 1$  and the volume to unity [26].

The fermions acquire self energy via pair binding and unbinding. Our approximated equations, derived via an equations of motion approach [42, 43], is often cast into a  $T$  matrix formalism, with a mix of bare Green's function  $G_0(K) = (i\omega_l - \xi_{\mathbf{k}})^{-1}$  and full Green's function  $G(K)$  in the pair susceptibility  $\chi(Q) = \sum_K G(K)G_0(Q - K)$ . Here we use the four-momentum notation,  $K \equiv (i\omega_n, \mathbf{k})$  and  $Q \equiv (i\Omega_l, \mathbf{q})$ ,  $\sum_K \equiv T \sum_{n,\mathbf{k}}$  and  $\sum_Q \equiv T \sum_{l,\mathbf{q}}$ , with  $\omega_n$  and  $\Omega_l$  being Matsubara frequencies for fermions and bosons, respectively [44]. The  $T$ -matrix  $t(Q)$  is given by  $t(Q) = U/[1 + U\chi(Q)]$ ,

with the self energy

$$\Sigma(K) = \sum_Q t(Q)G_0(Q - K).$$

The Thouless criterion (for superfluid transition in 3D) requires  $t^{-1}(Q = 0) = U^{-1} + \chi(0) = 0$ . In order to accommodate the absence of long range order in 2D, we generalize the Thouless criterion to allow for a very small but finite pair chemical potential  $\mu_p$ ,  $U^{-1} + \chi(0) = t^{-1}(0) \propto \mu_p$ . In this way,  $t(Q)$  is highly peaked around  $Q = 0$ . Thus the main contribution to  $\Sigma(K)$  comes from the vicinity of  $Q = 0$ , leading to a pseudogap approximation,  $\Sigma(K) \approx -\Delta^2 G_0(-K)$ , where we define the pseudogap as  $\Delta^2 = -\sum_Q t(Q)$ . With this approximation, the full Green's function takes a simple BCS-like form and is given by

$$G(K) = \frac{u_{\mathbf{k}}^2}{i\omega_n - E_{\mathbf{k}}} + \frac{v_{\mathbf{k}}^2}{i\omega_n + E_{\mathbf{k}}},$$

where  $E_{\mathbf{k}} = \sqrt{\xi_{\mathbf{k}}^2 + \Delta^2}$ ,  $u_{\mathbf{k}}^2 = (1 + \xi_{\mathbf{k}}/E_{\mathbf{k}})/2$ , and  $v_{\mathbf{k}}^2 = (1 - \xi_{\mathbf{k}}/E_{\mathbf{k}})/2$ . This leads to a BCS-like gap equation,

$$a_0\mu_p = \sum_{\mathbf{k}} \left[ \frac{1 - 2f(E_{\mathbf{k}})}{2E_{\mathbf{k}}} - \frac{1}{2\epsilon_{\mathbf{k}} + \epsilon_B} \right], \quad (1)$$

where  $a_0$  is the coefficient of the linear  $\Omega$  term in the Taylor expansion of the inverse  $T$ -matrix. Here the gap equation has been regularized via  $U^{-1} = -\sum_{\mathbf{k}} 1/(2\epsilon_{\mathbf{k}} + \epsilon_B)$ , where the two-body binding energy  $\epsilon_B = 1/ma_{2D}^2$  with the 2D scattering length  $a_{2D}$  [45]. The fermion number constraint  $n = 2\sum_{\mathbf{k}} G(K)$  yields

$$n = \sum_{\mathbf{k}} \left[ 1 - \frac{\xi_{\mathbf{k}}}{E_{\mathbf{k}}} + 2\frac{\xi_{\mathbf{k}}}{E_{\mathbf{k}}} f(E_{\mathbf{k}}) \right], \quad (2)$$

where  $f(x)$  is the Fermi distribution function.

To extract the pair dispersion, one Taylor-expands  $t^{-1}$  near  $Q = 0$  and analytically continues to real frequency, with  $(i\Omega_l \rightarrow \Omega + i0^+)$ , so that

$$t^{-1}(\Omega, \mathbf{q}) \approx a_1\Omega^2 + a_0(\Omega - \Omega_{\mathbf{q}}^0 + \mu_p), \quad (3)$$

where  $\Omega_{\mathbf{q}}^0 = \mathbf{q}^2/2M_B$ . Consequently, the definition of the pseudogap yields

$$n_B \equiv a_0\Delta^2 = \sum_{\mathbf{q}} \left[ 1 + 4\frac{a_1}{a_0}(\Omega_{\mathbf{q}}^0 - \mu_p) \right]^{-1/2} b(\Omega_{\mathbf{q}}), \quad (4)$$

where  $b(x)$  is the Bose distribution function and  $\Omega_{\mathbf{q}} = \left[ \sqrt{a_0^2 + 4a_0a_1(\Omega_{\mathbf{q}}^0 - \mu_p)} - a_0 \right] / 2a_1$  represents the pair dispersion. The coefficients  $a_0$ ,  $a_1$ ,  $M_B$  are determined via the expansion process. Except in the weak coupling BCS regime, the  $a_1$  term serves as a small quantitative correction and can often be neglected, so that  $\Omega_{\mathbf{q}} \approx \Omega_{\mathbf{q}}^0 - \mu_p$ . The way Eq. (4) yields  $n_B$  can be seen from the relation  $n_B = n/2 - \sum_{\mathbf{k}} f(\xi_{\mathbf{k}})$  [43].

## B. BKT Criterion

The Nelson-Kosterlitz condition (NKC) provides a criterion for determining  $T_{\text{BKT}}$ . However, there are issues with this condition. First of all, due to the Galilean translational invariance, one has the zero  $T$  superfluid density  $n_s(T = 0) = n$ , independent of the pairing strength. Furthermore, from the fermionic perspective, the fermion mass  $m$  is a constant. Hence it is hard to imagine that  $n_s(T_{\text{BKT}})/m$  would be able to properly capture the interaction effect. While it is often assumed  $M_B = 2m$  in a NKC-based calculation, however, the correct  $M_B$  should necessarily be renormalized by the interactions. Therefore, it is reasonable to suspect that NKC is not quantitatively reliable for a fermionic system.

Here we choose the criterion of critical phase space density  $\mathcal{D}_B$  to determine  $T_{\text{BKT}}$ , as established by Prokof'ev et al via quantum Monte Carlo (QMC) simulations of a Bose gas [25]. When approached from high temperature [4, 46], the bosonic BKT transition occurs when  $\mathcal{D}_B(T)$  reaches a critical value  $\mathcal{D}_B(T_{\text{BKT}})$  such that the boson wavefunctions start to overlap with each other [47]. Hence we have

$$\frac{n_B}{M_B} = \frac{\mathcal{D}_B}{2\pi} T_{\text{BKT}}, \quad (5)$$

where  $n_B$  and  $M_B$  are determined as described above. In the deep BEC regime, we have  $n_B = n/2$  and  $M_B = 2m$ , and hence the asymptotic behavior  $T_{\text{BKT}} = T_F/2\mathcal{D}_B$ . This would reduce to the NKC when  $\mathcal{D}_B = 4$ .

The critical phase space density  $\mathcal{D}_B$  has a very weak loglog dependence on  $a_{2D}$ , as given by  $\mathcal{D}_B = \ln(C/\tilde{g})$ , with  $C \approx 380$  [25]. Instead of using the expression for  $\tilde{g}$  in terms of potential range [25] or pair size [33], we take it directly from the experiment by fitting the data with the right form of function, which yields a perfect fit,

$$\tilde{g} = \frac{5.03085}{1.23629 - \ln(k_F a_{2D})}. \quad (6)$$

See App. B for details. The corresponding  $\mathcal{D}_B$  is given by the blue curve in Fig. 7. The fit also reveals that there exists a quantitative difference between  $a_{2D}$  and either the potential radius or the pair size.

The fit Eq. (6) is not to be applicable in the unitary and BCS regime. Since the relation  $\mathcal{D}_B = \ln(C/\tilde{g})$  no longer works well for the next available data point  $\tilde{g} = 7.55$  toward the unitary and BCS regimes [17], we set 4.9 as the lower bound for  $\mathcal{D}_B$  in the entire BCS-BEC crossover [48].

At  $T = 0$  where  $\mu_p = 0$ , Eqs. (1) and (2) give  $\mu = E_F - \epsilon_B/2$  and  $\Delta = \sqrt{2E_F\epsilon_B}$  [49]. At finite temperature, the summation in Eq. (4) analytically leads to  $\frac{a_0}{a_1} - \sqrt{\frac{a_0}{a_1}(\frac{a_0}{a_1} - 4\mu_p)} = 2T \ln(1 - e^{-\mathcal{D}_B})$ , which reduces to  $\mu_p = T \ln(1 - e^{-\mathcal{D}_B})$  in the BEC regime. Here use has been made of the relation  $\mathcal{D}_B = 2\pi n_B/M_B T$ . Thus  $\mu_p$  is primarily determined by  $\mathcal{D}_B$  at given temperature, indicating that when the BKT transition occurs  $\mathcal{D}_B$  is large enough so that  $\mu_p$  becomes sufficiently close to zero [17, 18, 24, 47]. Moreover, in the BEC regime, a large  $\mathcal{D}_B$  provides a sharp peak distribution of the bosonic

number density at zero momentum via  $b(-\mu_p) = e^{\mathcal{D}_B} - 1$ , signaling a quasi-condensation [24]. Alternatively, when  $\mathcal{D}_B(T)$  becomes large enough, the wave functions of neighboring pairs start to overlap with each other, and hence help to establish quasi-long-range phase coherence.

### C. Contributions of the Particle-Hole Channel

Following Ref. [32], we introduce the contribution of the particle-hole channel, by renormalizing the pairing strength in  $t(Q)$ , which leads to a new full  $T$ -matrix  $t_2(Q)$  that includes both particle-particle and particle-hole contributions. The expression for  $t_2(Q)$  is formally given by

$$t_2(Q) = \frac{1}{t_{\text{ph}}^{-1}(K + K' - Q) + \chi(Q)},$$

which self-consistently includes the self-energy feedback, with  $K, K'$  being the external fermion momentum. Here the particle-hole channel  $T$  matrix  $t_{\text{ph}}^{-1}(Q') = U^{-1} + \chi_{\text{ph}}(Q')$  describes the particle-hole scattering, and the particle-hole susceptibility  $\chi_{\text{ph}}(Q') = \sum_K G(K)G_0(K - Q')$ , where the particle-hole momentum  $Q' = K + K' - Q$ . Moreover, assuming that the fermions near the Fermi surface dominate the particle-hole channel contributions, we replace the particle-hole susceptibility with an average  $\langle \chi_{\text{ph}} \rangle$  on or near the Fermi surface, where the frequency part of the particle-hole susceptibility is set to 0 with  $i\Omega'_n = 0$  [50], leading to a zero imaginary part of  $\chi_{\text{ph}}(Q')$  and therefore a purely real  $\langle \chi_{\text{ph}} \rangle$  [32].

We have proposed two methods for averaging  $\chi_{\text{ph}}(Q')$ , referred to as level 1 and level 2, respectively. The level 1 average involves an on-shell and elastic scattering on the Fermi surface, with  $|\mathbf{k}| = |\mathbf{k}'| = k_\mu = \sqrt{2m} \max(\mu, 0)$ , where the momentum part of  $\chi_{\text{ph}}(Q')$  is determined by  $|\mathbf{q}'| = |\mathbf{k} + \mathbf{k}'| = k_\mu \sqrt{2(1 + \cos\theta)}$ . Here  $\chi_{\text{ph}}(Q')$  is averaged over scattering angles  $\theta$  (between  $\mathbf{k}$  and  $\mathbf{k}'$ ). This averaging process, focusing solely on the Fermi surface, is commonly used in the literature on the studies of induced interactions [31]. In contrast, the level 2 average considers that the states within the energy range  $\xi_{\mathbf{k}} \in [-\min(\Delta, \mu), \Delta]$  of a typical s-wave superconductor are most significantly affected by pairing (for  $\mu > 0$ ). Hence, for the level 2 average, while keeping the on-shell and elastic scattering assumption, the average is performed over a range of  $|\mathbf{k}|$  such that the quasi-particle energy  $E_{\mathbf{k}} \in [\min(E_{\mathbf{k}}), \min(\sqrt{E_{\mathbf{k}}^2 + \Delta^2})]$ , where  $\min(E_{\mathbf{k}}) = \Delta$  if  $\mu > 0$ , or  $\min(E_{\mathbf{k}}) = \sqrt{\mu^2 + \Delta^2}$  if  $\mu < 0$ .

Then with this frequency and momentum independent  $\langle \chi_{\text{ph}} \rangle$ , the new full  $T$ -matrix  $t_{\text{eff}}(Q)$  reads

$$t_{\text{eff}}(Q) = \frac{1}{U^{-1} + \langle \chi_{\text{ph}} \rangle + \chi(Q)}. \quad (7)$$

The gap equation with the particle-hole channel effect is modified into

$$a_0 \mu_p = \langle \chi_{\text{ph}} \rangle + \sum_{\mathbf{k}} \left[ \frac{1 - 2f(E_{\mathbf{k}})}{2E_{\mathbf{k}}} - \frac{1}{2\epsilon_{\mathbf{k}} + \epsilon_B} \right], \quad (8)$$

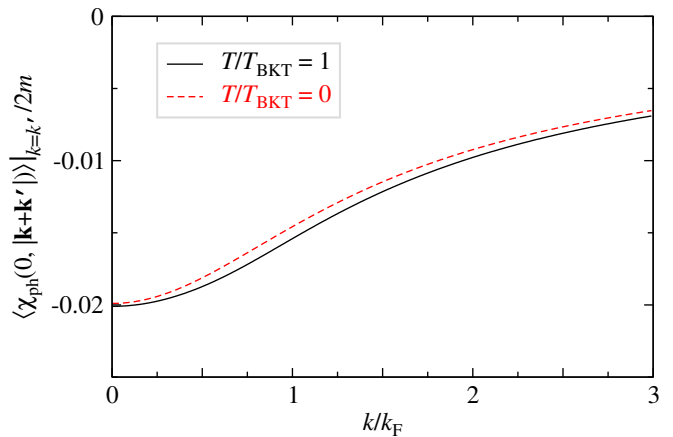


Figure 1. Angular average of the on-shell particle-hole susceptibility  $\langle \chi_{\text{ph}}(0, |\mathbf{k} + \mathbf{k}'|) \rangle / 2m$  with  $k = k'$  as a function of momentum  $k/k_F$  at unitarity  $\ln(k_F a_{2D}) = 0$  for  $T = 0$  and  $T = T_{\text{BKT}}$ , where  $T_{\text{BKT}}/T_F = 0.079$  and the corresponding  $\Delta, \mu$  and  $\mu_p$  are calculated without the particle-hole channel effect.

while the other equations remain unchanged.

Equations (2), (4), and (8) form a closed set of self-consistent equations, which can be used to solve for  $(\mu, \Delta, \mu_p)$ , along with  $T_{\text{BKT}}$  via the BKT criterion given by Eq. (5).

Throughout the BCS-BEC crossover,  $\langle \chi_{\text{ph}} \rangle$  remains negative as a function of the coupling strength. From Eq. (8), the particle-hole channel constitutes a renormalization of the pairing interaction, with a net effect given by replacing  $1/U$  with  $1/U_{\text{eff}} \equiv 1/U + \langle \chi_{\text{ph}} \rangle$ . Diagrammatically, this amounts to replacing the bare interaction  $U$  with the full particle-hole  $T$ -matrix  $t_{\text{ph}}$  in the particle-particle scattering diagrams [32]. Since  $\langle \chi_{\text{ph}} \rangle < 0$ , one has  $|U_{\text{eff}}| < |U|$ . Thus  $U_{\text{eff}}$  represents a weaker, screened pairing interaction.

## III. NUMERICAL RESULTS AND DISCUSSIONS

### A. Behaviors of the particle-hole susceptibility

First, we present in Fig. 1 the (level 1) angular average of the particle-hole susceptibility at zero frequency as a function of momentum  $k$ , under the on-shell condition  $|\mathbf{k}| = |\mathbf{k}'| = k$ . Here we focus on the unitary case at  $T = T_{\text{BKT}}$  (black solid line) and zero-temperature (red dashed line), and  $\langle \chi_{\text{ph}}(0, |\mathbf{k} + \mathbf{k}'|) \rangle$  is calculated using the corresponding solution of  $(\Delta, \mu, \mu_p)$  at  $T_{\text{BKT}}/T_F = 0.079$  and  $\ln(k_F a_{2D}) = 0$ , solved in the absence of particle-hole fluctuations. The slight difference between these two curves reveals a weak temperature dependence. Importantly, both curves show a significant momentum dependence, with the amplitude decreasing monotonically as the momentum rises. Note that the momentum dependencies in 2D appear distinct from those in 3D [32], where  $\langle \chi_{\text{ph}}(0, |\mathbf{k} + \mathbf{k}'|) \rangle$  exhibits a nonmonotonic momentum dependence at low  $T$  for the unitary case.

Shown in Fig. 2 is  $-\langle \chi_{\text{ph}} \rangle$  at  $T = T_{\text{BKT}}$  as a function of

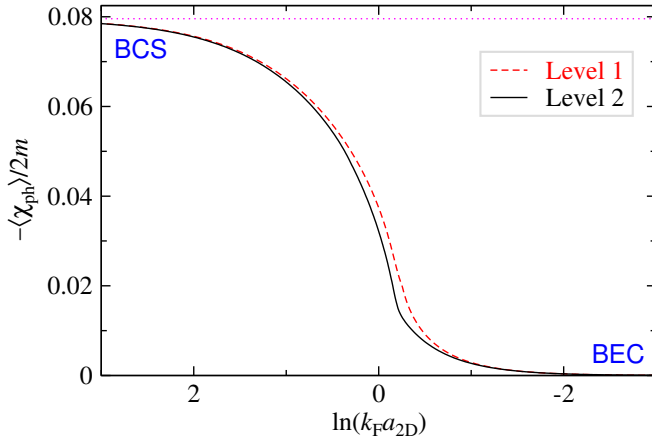


Figure 2.  $-\langle\chi_{\text{ph}}\rangle/2m$  at  $T = T_{\text{BKT}}$ , averaged at both level 1 (red dashed) and level 2 (black solid line), as a function of  $\ln(k_F a_{2D})$  throughout BCS-BEC crossover. The magenta dotted line indicates the BCS limit value,  $1/4\pi$ , given by  $-\langle\chi_{\text{ph}}\rangle = m/2\pi$ .

$\ln(k_F a_{2D})$  throughout the BCS-BEC crossover, averaged at both level 1 (red dashed) and level 2 (black solid curve), along with its BCS limit  $1/4\pi \approx 0.0796$ , given by  $\langle\chi_{\text{ph}}\rangle = -m/2\pi$ . The value of  $-\langle\chi_{\text{ph}}\rangle/2m$  decreases monotonically with increasing interaction strength and exhibits an exponential behavior in the deep BEC regime for  $\ln(k_F a_{2D}) < -2$ . As the gap diminishes, the average at both levels converges in the BCS limit. However, in the crossover regime, the two levels differ significantly, with a smaller absolute value for the level 2 average. This can be understood from Fig. 1; compared with level 1 averaging, level 2 averaging involves a range of  $k$ 's so that the larger  $k$  contributions dominate due to its larger phase space area, leading to a smaller absolute value of the average. In other words, level 1 averaging on the Fermi surface only leads to a significant over-estimate of the particle-hole contributions in the unitary regime.

The asymptotic behavior of  $\langle\chi_{\text{ph}}\rangle$  can be readily solved analytically in both the BCS and the BEC limits. In the weak coupling limit, where  $\ln(k_F a_{2D}) \rightarrow \infty$ ,  $\Delta \rightarrow 0$ , and  $T_{\text{BKT}} \rightarrow 0$ , the two levels of average converge to  $\chi_{\text{ph}}(Q') \approx \sum_K G_0(K)G_0(K - Q')$ . Under the on-shell condition  $\xi_{\mathbf{k}} = \xi_{\mathbf{k}-\mathbf{q}'}$ , the integrand becomes the derivative of the Fermi function and one readily obtains

$$\chi_{\text{ph}}(0, \mathbf{q}') = \sum_{\mathbf{k}} \frac{f(\xi_{\mathbf{k}}) - f(\xi_{\mathbf{k}-\mathbf{q}'})}{\xi_{\mathbf{k}} - \xi_{\mathbf{k}-\mathbf{q}'}} \approx -\frac{m}{2\pi} = \langle\chi_{\text{ph}}\rangle. \quad (9)$$

We emphasize that this result is independent of the density, due to the constant density of states in 2D. This is to be contrasted with its 3D counterpart, which is proportional to the Fermi momentum  $k_F$ . In the strong coupling limit, where  $\ln(k_F a_{2D}) \rightarrow -\infty$ , we have  $|\mu| \gg \Delta \gg E_F$ , so that  $E_{\mathbf{k}} \approx \xi_{\mathbf{k}} \approx |\mu|$ . Thus particle-hole fluctuations are exponentially suppressed, so that  $\langle\chi_{\text{ph}}\rangle$  approaches zero.

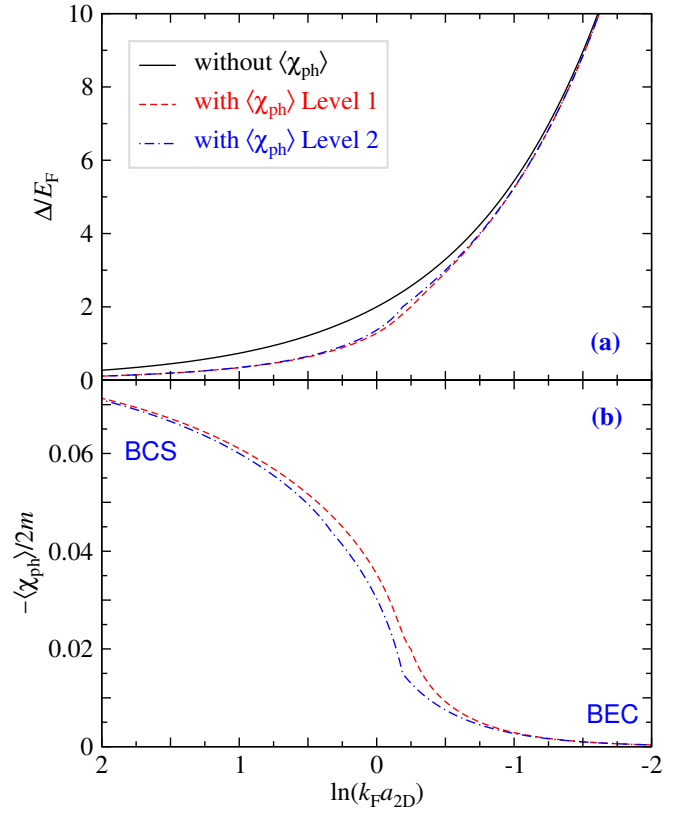


Figure 3. (a) Effect of the particle-hole channel contributions on  $\Delta$ , along with (b) the corresponding  $-\langle\chi_{\text{ph}}\rangle/2m$ , at  $T = 0$ , as a function of  $\ln(k_F a_{2D})$  throughout the BCS-BEC crossover. Shown are results without (black solid curve) and with particle-hole channel contributions averaged at level 1 (red dashed) and level 2 (blue dot-dashed curve).

## B. Effect of the particle-hole channel on BKT transition

In this section, we explore the impact of the particle-hole channel on the pairing phenomena and the BKT transition of a 2D Fermi gas. We begin by examining the behavior of the pairing gap  $\Delta$  at zero temperature with and without the particle-hole channel contributions. Plotted in Fig. 3(a) is  $\Delta$  as a function of interaction, parameterized by  $\ln(k_F a_{2D})$ . For comparison, we plot the results both without (black solid line) and with the particle-hole channel effect, with the particle-hole susceptibility  $\langle\chi_{\text{ph}}\rangle$  averaged at level 1 (red dashed curve) and level 2 (blue dot-dashed curve), respectively. The corresponding  $\langle\chi_{\text{ph}}\rangle$  is shown in Fig. 3(b). Compared to Fig. 2, the difference in  $\langle\chi_{\text{ph}}\rangle$  is larger at  $T = 0$  than at  $T = T_{\text{BKT}}$ . For all cases,  $\Delta$  increases monotonically from BCS to BEC, as expected. A substantial reduction of  $\Delta$  by the particle-hole fluctuations occurs in the crossover and BCS regimes. In the BEC regime,  $\langle\chi_{\text{ph}}\rangle$  approaches zero, rendering the particle-hole channel effect negligible. Consistent with Fig. 3(b), level 2 averaging showed a weaker particle-hole effect, and thus a smaller reduction of  $\Delta(T = 0)$ . Note that in Fig. 3(b), there exists a kink where  $\mu = 0$  in  $\langle\chi_{\text{ph}}\rangle$  for both levels of averaging, mainly because the Fermi surface shrinks to zero abruptly

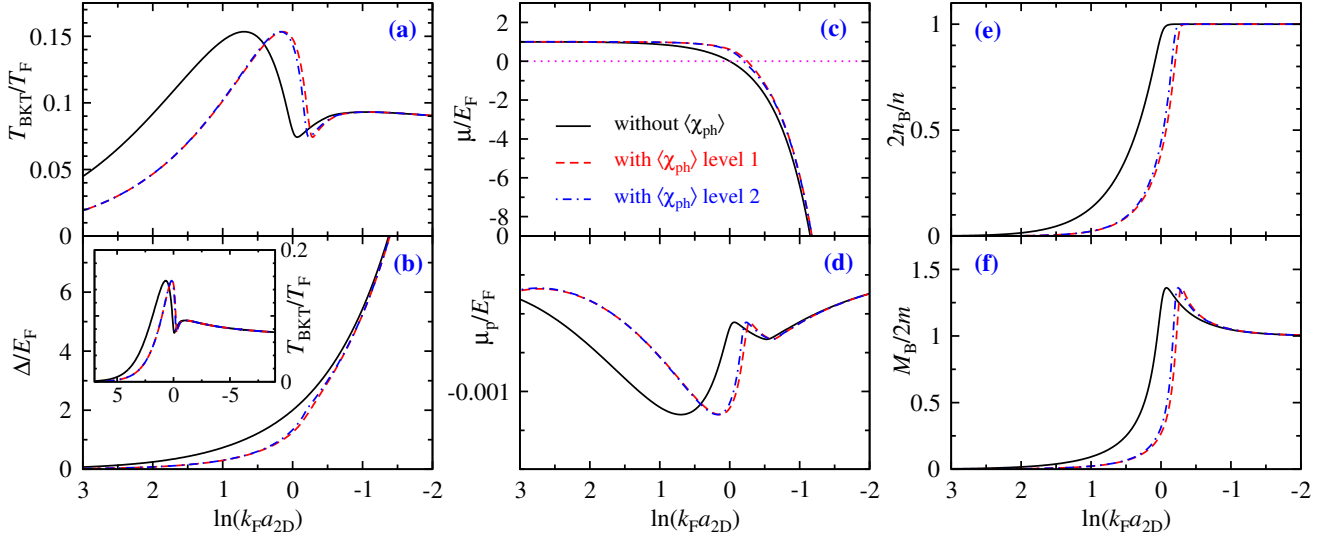


Figure 4. Effect of the particle-hole channel on (a)  $T_{\text{BKT}}$ , (b)  $\Delta$ , (c)  $\mu$ , (d)  $\mu_p$ , (e)  $n_B$  and (f)  $M_B$  as a function of  $\ln(k_F a_{2D})$ , with the average  $\langle \chi_{\text{ph}} \rangle / 2m$  calculated at level 1 (red dashed) and level 2 (blue dot-dashed curves), respectively. They should be compared with the results without the particle-hole contributions (black solid curves). Shown in the inset of (b) is  $T_{\text{BKT}}$  over a broader range. The difference between levels 1 and 2 is not dramatic.

with a finite slope as a function of increasing pairing strength. The Fermi function in the integrand of  $\langle \chi_{\text{ph}} \rangle$  becomes a step function at zero  $T$ , resulting in a Dirac delta function in the derivative of the integrand of  $\langle \chi_{\text{ph}} \rangle$  and hence a slope discontinuity when crossing  $\mu = 0$  (See Appendix A for details). This slope discontinuity becomes more prominent in the level 2 average, since the range for  $k < k_\mu$  in the average also shrinks to zero abruptly when  $\mu = 0$  [51].

For the effect of the particle-hole channel on the behavior of the BKT transition temperature  $T_{\text{BKT}}$ , we first analytically estimate the ratio between the two BKT transition temperatures in the BCS limit with and without the particle-hole channel at the same coupling strength, where the latter is denoted as  $T_{\text{BKT}}^{\text{BCS}}$ . Now that  $\Delta \rightarrow 0$ , we obtain

$$\sum_{\mathbf{k}} \left[ \frac{1 - 2f(\xi_{\mathbf{k}})}{2\xi_{\mathbf{k}}} - \frac{1}{2\epsilon_{\mathbf{k}} + \epsilon_B} \right] = \frac{m}{4\pi} \ln \left( \frac{2e^{2\gamma} \epsilon_B E_F}{\pi^2 T^2} \right),$$

where  $\gamma \approx 0.5772157$  is Euler's constant. Substituting the above relation for the corresponding term in Eqs. (1) and (8), we obtain

$$\frac{T_{\text{BKT}}}{T_{\text{BKT}}^{\text{BCS}}} = e^{2\pi \langle \chi_{\text{ph}} \rangle / m} = e^{-1} \approx 0.37,$$

where we have taken into account that  $t^{-1}(0)$  and  $t_2^{-1}(0)$  are sufficiently small so that  $|t^{-1}(0)|, |t_2^{-1}(0)| \ll |\langle \chi_{\text{ph}} \rangle|$  in the weak coupling limit.

Next, we present in Fig. 4 the effect of the particle-hole channel on the evolution of (a)  $T_{\text{BKT}}$ , along with (b)  $\Delta$ , (c)  $\mu$ , (d)  $\mu_p$ , (e)  $n_B$ , and (f)  $M_B$  at  $T_{\text{BKT}}$  as a function of  $\ln(k_F a_{2D})$ . Shown in the inset is  $T_{\text{BKT}}$  over a broad range of  $\ln(k_F a_{2D})$ . For comparison, the results without particle-hole fluctuations are presented as the black solid curves. Consider the case

without particle-hole effects first. Starting from the weak coupling BCS limit (black curve), as the interaction strength increases,  $T_{\text{BKT}}$  increases, and then reaches a maximum around  $\ln(k_F a_{2D}) = 0.7$  in the intermediate regime, where  $\mu_p$  reaches a minimum simultaneously. The fact there appears a maximum reflects that  $n_B$  rises faster than  $M_B$  in this regime (see (e,f)). As the interaction strength increases further past the maximum,  $T_{\text{BKT}}$  decreases and reaches a minimum near unitarity  $\ln(k_F a_{2D}) = 0$ , where  $\mu = 0$ . Beyond this point, the system enters the BEC regime, where all fermions pair up with  $2n_B/n \approx 1$ , as shown in Fig. 4(e). The behavior of  $T_{\text{BKT}}$  is then dominated by the shrinking pair size, as indicated by a decrease in the pair mass  $M_B$  toward  $2m$  (Fig. 4(f)), reaching the BEC asymptotic behavior  $T_{\text{BKT}}/T_F = 1/2\mathcal{D}_B$  governed by Eq. (5). This decreasing  $M_B$  leads to an increase and hence a minimum in  $T_{\text{BKT}}$ . The gap  $\Delta$  in Fig. 4(b) increases consistently with pairing strength. In comparison, the particle-hole contributions cause a *non-uniform shift* of all curves toward the BEC regime on the right. This shift is the largest in the BCS limit, and vanishes in the BEC regime, as indicated in Fig. 2. It exhibits a strong dependence on  $\ln(k_F a_{2D})$  in the crossover regime. Now the maximum of  $T_{\text{BKT}}$  occurs closer to unitarity, and the location for  $\mu = 0$  is shifted into the previous BEC regime. All  $T_{\text{BKT}}$  curves with and without the particle-hole effect converge to the same BEC asymptotic curve, since the particle-hole contributions vanish gradually in the BEC regime. From Fig. 4(d), we see a tiny  $|\mu_p| \leq 1.2 \times 10^{-3} E_F$  throughout the BCS-BEC crossover for all cases. Especially, in the BEC regime, it is uniquely determined by  $\mathcal{D}_B$ . This ensures that  $t(Q)$  remains highly peaked at  $Q = 0$  and thus validates our pseudogap approximation for the self-energy.

Now we investigate in Fig. 5 the evolution of  $\Delta$  (top row) and  $\mu_p$  (bottom row) as a function of reduced temperature  $T/T_{\text{BKT}}$  in the BCS, unitary, and BEC regimes from left to

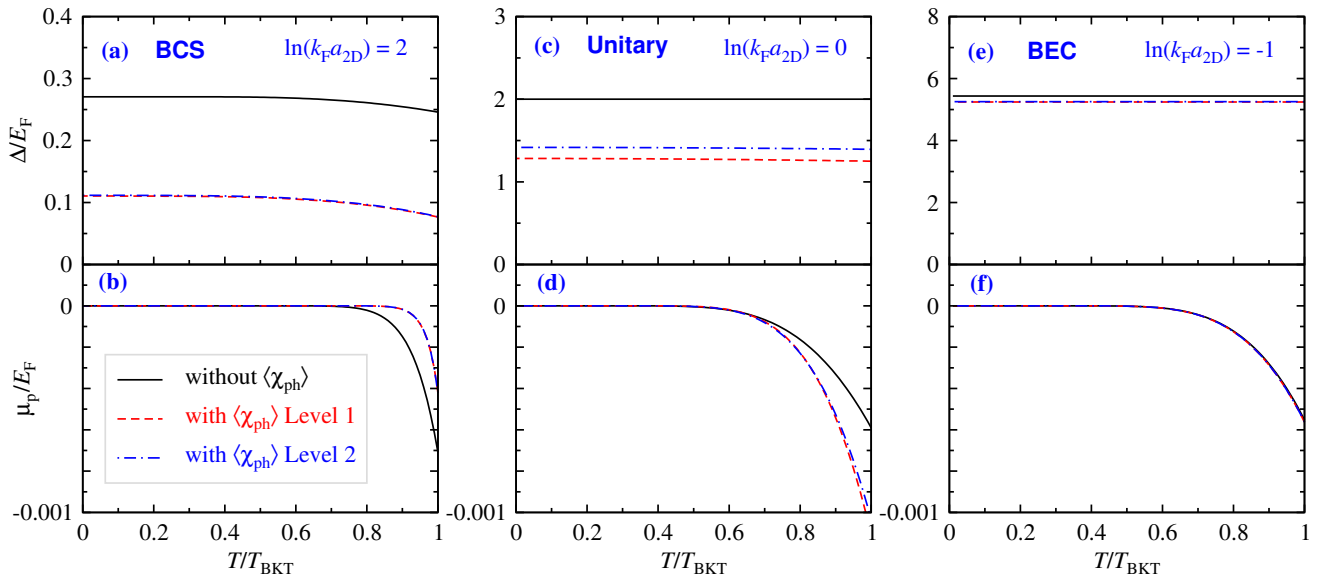


Figure 5. Effect of the particle-hole channel contributions on behaviors of  $\Delta$  (top row) and  $\mu_p$  (bottom row), as a function of  $T/T_{\text{BKT}}$ , with  $\ln(k_F a_{2D}) = 2, 0, -1$  from left to right for the BCS, unitary, and BEC regimes, respectively. The black solid curves represent calculations without the particle-hole channel, while the red dashed and green dot-dashed curves include the particle-hole channel effect, using  $\langle\chi_{\text{ph}}\rangle/2m$  under level 1 and level 2 averaging, respectively.

right without (black) and with (red and green) the particle-hole channel effect. The gap  $\Delta$  remains nearly constant except in the BCS case (a), where a significant decrease can be discerned near  $T_{\text{BKT}}$ . The pseudogap  $\Delta$  with the particle-hole channel effect is reduced from the counterpart without the particle-hole effect by a factor of  $1/e$  in the BCS limit. This reduction factor becomes smaller in the unitary and BEC regimes, consistent with the zero  $T$  and  $T_{\text{BKT}}$  gap behaviors shown in Fig. 3(a) and Fig. 4(b). At the same time, for all cases,  $\mu_p$  increases continuously to zero as  $T$  decreases, consistent with  $\mu_p = 0$  at  $T = 0$  for a true long-range-ordered ground state. Note that below  $0.6T_{\text{BKT}}$ ,  $\mu_p$  comes essentially zero. Interestingly,  $|\mu_p|$  decreases much faster with decreasing  $T$  in the BCS regime than in the unitary and BEC regimes. Conversely, should the calculation be extended to above  $T_{\text{BKT}}$ ,  $|\mu_p|$  would rise rapidly with  $T$  so that pairs would quickly become irrelevant in this regime.

### C. Comparison with different results

Finally, in Fig. 6, we compare our theoretical  $T_{\text{BKT}}$  with available experimental data [16] and QMC results, as well as other theories where appropriate, on the BKT transition in 2D Fermi gases, as a function of  $\ln(k_F a_{2D})$  throughout the BCS-BEC crossover. Figure 6(a) presents the measured quasi-condensate fractions  $N_q/N$  [16], overlaid on top of which are the theory curves calculated using our pairing fluctuation theory without (black solid) and with (light cyan solid curve) the particle-hole contributions (level 1). The black solid line was previously presented in Ref. [18], calculated with a fixed  $\mathcal{D}_B = 4.9$ . The experimental data are not dense enough to enable a successful detection of the minimum in

$T_{\text{BKT}}$  near  $\ln(k_F a_{2D}) = 0$ , nevertheless, it does seem to suggest there exists a minimum in this neighborhood in the contour of the quasi-condensate fraction. Thus, our theory is consistent with the data, including the presence of the minimum. Our present curve does align better with the slightly decreasing  $T_{\text{BKT}}$  and contour of the quasi-condensate fraction toward BEC. In Fig. 6(b), we compare our  $T_{\text{BKT}}$  with a collection of other theories [21–23, 33], and results obtained from QMC using a 2D lattice model [53]. Also plotted are the experimental results from Refs. [16] and [52]. In the BEC regime, where particle-hole contributions become negligible, our results both with (black solid) and without (black dashed line) are in quantitative agreement with both experiments, as well as that of Petrov et al [33]. Here we choose to show only the result with level 1 average of the particle-hole susceptibility, giving the relatively small quantitative difference in  $T_{\text{BKT}}$  between levels 1 and 2. There is an expected small difference between Petrov et al [33] and our present result based on experimental  $\mathcal{D}_B$ , due to the quantitative difference between the pair size used in Ref. [33] and the scattering length  $a_{2D}$ . In the BCS regime, the curves of Mulkerin et al [23] and of the BCS mean-field treatment are close to our curve without particle-hole, suggesting that particle-hole contributions are not included in Mulkerin et al [23]. Our particle-hole corrected result (black solid curve) is in good agreement with the QMC result extrapolated to the infinite  $L$  limit, except that QMC does not show a minimum in the unitary regime [53]. For  $\ln(k_F a_{2D}) > 2$ , the QMC for infinite lattice size  $L$  does not have data points, while the results of Petrov et al [33] starts to merge with our (black solid) particle-hole corrected curve. In comparison, Bauer et al [21] has a higher  $T_{\text{BKT}}$  in this regime; their curve intersects with the curves of our particle-hole corrected result, Petrov et al and QMC (infinite  $L$ ). We also notice a large difference between

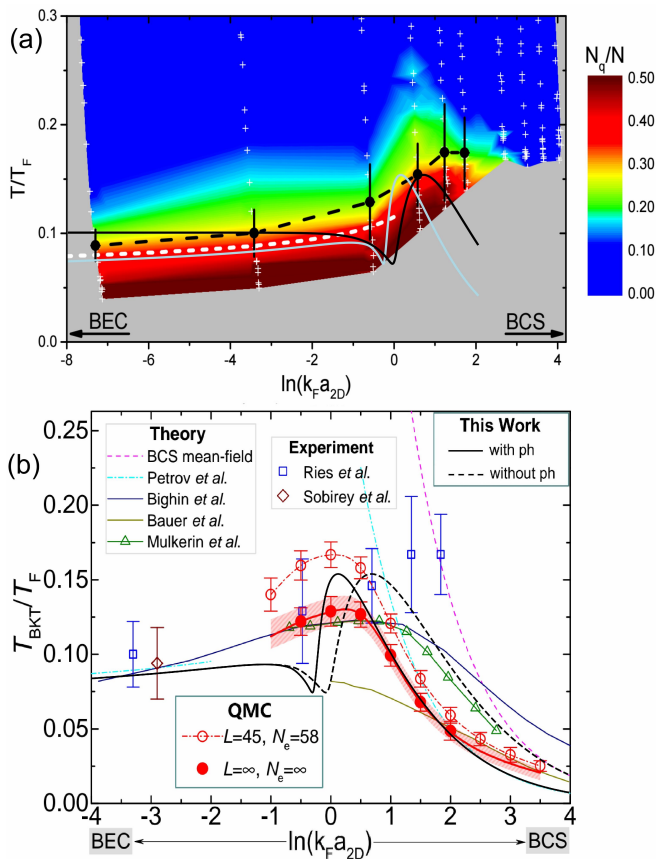


Figure 6. Comparison of theoretical calculations for  $T_{\text{BKT}}/T_F$  with experiment [16, 52] and QMC [53] results as a function of  $\ln(k_F a_{2D})$  throughout the BCS-BEC crossover. (a) Overlay of theoretical  $T_{\text{BKT}}$  without (black solid line, with fixed  $\mathcal{D}_B = 4.9$  from Ref. [18]) and with the particle-hole channel calculated with the level 1 average of experimentally measured quasi-condensate fractions [16]. Adapted from Ref. [18]. (b) Overlay of our  $T_{\text{BKT}}$  on top of a collection of experimental data [16, 52], QMC [53] and various theoretical results [21–23, 33]. The black solid and dashed lines represent  $T_{\text{BKT}}$  calculated using our pairing fluctuation theory with and without the particle-hole channel contributions, respectively. Here the particle-hole channel effect was calculated with level 1 averaging of  $\langle \chi_{\text{ph}} \rangle$ . Adapted from Ref. [53].

the finite ( $L = 45$ ) and infinite lattice QMC results. It is unusual that the result of Bighin *et al.* [22] is far above the BCS mean-field value in the BCS limit [54]. They also ignored the particle-hole contributions. It should be noted that the experimental data in the BCS regime are significantly above all theory curves, except the mean-field result; no sign of decrease toward the BCS regime can be discerned. This suggests that some other factors, e.g., nonequilibrium, finite size effect, need to be considered. Therefore, we shall refrain from comparing with these experimental data in the BCS regime. In short, our results with the particle-hole contributions are consistent with experiment in the unitary and BEC regimes and in good agreement with the QMC results [53] in the unitary and BCS regimes. This calls for more data from future experiment.

A few remarks are in order. (i) In the BCS limit, the bosonic fluctuation contributions are relatively weak. The mean-field superfluid density  $n_s/m$  has a strong temperature dependence and decreases sharply toward zero at the mean-field transition temperature  $T_c^{\text{MF}}$ . Any fluctuation effect would only suppress  $n_s/m$ . Therefore, it serves to provide an upper bound for  $T_{\text{BKT}}$ . The sharp  $T$  dependence of  $n_s/m$  (and  $n_B/M_B$ ) near  $T_c^{\text{MF}}$  implies that one has  $T_{\text{BKT}} \lesssim T_c^{\text{MF}}$ , insensitive to the actual condition used. (ii) It is well known that, in the continuum, one has  $n_s(T=0)/m = n/m$  due to the Galilean translational invariance. For this reason, Shi *et al.* [19] presented an interaction-independent upper bound  $T_F/8$  for  $T_{\text{BKT}}$ . Thus it is hard to imagine that  $n_s(T = T_{\text{BKT}})/m$  would properly reflect the effect of inter-fermion interactions. In this sense, we suspect that the NKC cannot properly capture the interaction effect in the crossover regime of a fermionic superfluid system. (iii) Furthermore, in an NKC-based approach [22, 23], it is often assumed  $M_B = 2m$  throughout the BCS-BEC crossover, ignoring possible pair mass renormalization. (iv) Therefore, the non-monotonic behavior of  $T_{\text{BKT}}$  we find in Fig. 4(a) is unlikely to be present in an NKC-based calculation.

Finally, we note that the particle-hole susceptibility in Eq. (9) is density independent in 2D. This suggests that the particle-hole contributions in the weak coupling limit would have already been automatically included, if the 2D scattering length  $a_{2D}$  were measured directly through experiment, e.g., by measuring the two-body binding energy in the dilute limit. Instead,  $a_{2D}$  is usually calculated from the 3D scattering length as in a deeply confined pancake-shaped trap [55], thus the effect of particle-hole fluctuations should be seriously taken into account when comparing experiment and theory. In Fig. 6, the same definition of  $a_{2D}$  was used in both QMC and our present work. This makes it possible to have a good agreement in the BCS regime between QMC and our result with particle-hole fluctuations included. Conversely, one can experimentally determine the particle-hole susceptibility in the BCS limit by measuring the 2D scattering length and comparing with that calculated from  $a_{3D}$ , and obtain

$$\langle \chi_{\text{ph}} \rangle = \frac{m}{2\pi} \ln \frac{a_{2D}^{\text{exp}}}{a_{2D}},$$

where  $a_{2D}^{\text{exp}}$  denotes the experimentally measured 2D scattering length. Nevertheless, away from the weak coupling limit, a nontrivial density dependence should emerge as both a nonzero pairing gap develops and the ratio  $\mu/E_F$  starts to decrease with increasing pairing strength at a finite density.

#### IV. CONCLUSIONS

In summary, we have studied the impact of the particle-hole channel on the BKT physics in Fermi gases within the context of BCS-BEC crossover. The entire particle-hole  $T$  matrix is included to renormalize the interaction that appears in the particle-particle  $T$  matrix. Both  $T$  matrices contain self-consistently includes the self-energy feedback. This leads

to a non-uniform shift of the inverse interaction strength by the particle-hole susceptibility, which evaluated as an angular average at two different levels, revealing important physical consequences in the crossover and BCS regimes. The particle-hole channel provides a screening of the pairing interaction and thus shifts curves of the BKT transition temperature and the pairing gap towards the BEC regime as a function of  $\ln(k_F a_{2D})$ . Additionally, a comparison shows that the particle-hole corrected BKT transition temperature exhibits a better agreement with the experimental data and QMC results. Future experiments with more elaborate measurements are called for to resolve various discrepancies.

Finally, it should be mentioned that, in addition to the simple averaged particle-hole susceptibility, there are a series of higher order corrections, including a higher order  $T$ -matrix [32] and vertex corrections, which may contribute significant modifications to the present results. In addition, the BKT criterion [18, 24] is merely based on numerical simulations [25] to provide the critical phase space density. Despite the experimental support [17], a rigorous analytical derivation of such a criterion would be highly desirable.

## V. ACKNOWLEDGMENTS

This work was supported by the Innovation Program for Quantum Science and Technology (Grant No. 2021ZD0301904).

### Appendix A: Slope discontinuity in $\chi_{\text{ph}}$ across $\mu = 0$ at zero $T$

The expression for the particle-hole susceptibility  $\chi_{\text{ph}}(Q')$  is given by

$$\chi_{\text{ph}}(Q') = \sum_{\mathbf{k}} \left[ \frac{f(E_{\mathbf{k}}) - f(\xi_{\mathbf{k}-\mathbf{q}'})}{E_{\mathbf{k}} - \xi_{\mathbf{k}-\mathbf{q}'} - i\Omega'_n} u_{\mathbf{k}}^2 - \frac{1 - f(E_{\mathbf{k}}) - f(\xi_{\mathbf{k}-\mathbf{q}'})}{E_{\mathbf{k}} + \xi_{\mathbf{k}-\mathbf{q}'} + i\Omega'_n} v_{\mathbf{k}}^2 \right].$$

Upon analytical continuation,  $i\Omega'_n \rightarrow \Omega' + i0^+$ , we separate the retarded  $\chi_{\text{ph}}^R(\Omega', \mathbf{q}')$  into real and imaginary parts,  $\chi_{\text{ph}}^R(\Omega', \mathbf{q}') = \chi'_{\text{ph}}(\Omega', \mathbf{q}') + i\chi''_{\text{ph}}(\Omega', \mathbf{q}')$ . Furthermore, we set  $i\Omega'_n = 0$ , which leads to  $\chi''_{\text{ph}}(0, \mathbf{q}') = 0$ , and the real part is expressed as

$$\chi'_{\text{ph}}(0, \mathbf{q}') = \sum_{\mathbf{k}} \left[ \frac{f(E_{\mathbf{k}}) - f(\xi_{\mathbf{k}-\mathbf{q}'})}{E_{\mathbf{k}} - \xi_{\mathbf{k}-\mathbf{q}'}} u_{\mathbf{k}}^2 - \frac{1 - f(E_{\mathbf{k}}) - f(\xi_{\mathbf{k}-\mathbf{q}'})}{E_{\mathbf{k}} + \xi_{\mathbf{k}-\mathbf{q}'}} v_{\mathbf{k}}^2 \right].$$

At  $T = 0$ , we have  $f(x) = 1 - \Theta(x)$ . Thus  $\chi'_{\text{ph}}(0, \mathbf{q}')$  is given by

$$\chi'_{\text{ph}}(0, \mathbf{q}') = \sum_{\mathbf{k}} \left[ \frac{\Theta(\xi_{\mathbf{k}-\mathbf{q}'}) - 1}{E_{\mathbf{k}} - \xi_{\mathbf{k}-\mathbf{q}'}} u_{\mathbf{k}}^2 - \frac{\Theta(\xi_{\mathbf{k}-\mathbf{q}'})}{E_{\mathbf{k}} + \xi_{\mathbf{k}-\mathbf{q}'}} v_{\mathbf{k}}^2 \right].$$

Then the derivative of  $\chi'_{\text{ph}}(0, \mathbf{q}')$  with respect to  $\mu$  is given by

$$\begin{aligned} \frac{\partial}{\partial \mu} \chi'_{\text{ph}}(0, \mathbf{q}') &= - \sum_{\mathbf{k}} \left[ \frac{1 + \delta(\xi_{\mathbf{k}-\mathbf{q}'})}{E_{\mathbf{k}} + \xi_{\mathbf{k}-\mathbf{q}'}} v_{\mathbf{k}}^2 - \frac{\delta(\xi_{\mathbf{k}-\mathbf{q}'})}{E_{\mathbf{k}} - \xi_{\mathbf{k}-\mathbf{q}'}} u_{\mathbf{k}}^2 \right] \\ &= \begin{cases} - \sum_{\mathbf{k}} \frac{v_{\mathbf{k}}^2}{E_{\mathbf{k}} + \xi_{\mathbf{k}-\mathbf{q}'}} , & \mu < 0, \\ - \sum_{\mathbf{k}} \frac{v_{\mathbf{k}}^2}{E_{\mathbf{k}} + \xi_{\mathbf{k}-\mathbf{q}'}} + \sum_{\phi \in A} \frac{\xi_{\mathbf{k}'}}{E_{\mathbf{k}'}} , & \mu \geq 0, \end{cases} \end{aligned}$$

where  $A = \{\phi : p^2(\cos(\phi)^2 - 1)/2 + \mu\}$  with  $\mathbf{k}' = p \cos(\phi) \pm \sqrt{p^2(\cos(\phi)^2 - 1)/2 + \mu}$  given by  $\xi_{\mathbf{k}-\mathbf{q}'} = 0$ . Thus, an additional term in the derivative of  $\chi'_{\text{ph}}(0, \mathbf{q}')$  emerges when the system changes from  $\mu < 0$  to  $\mu \geq 0$ , leading to a slope discontinuity of  $\chi_{\text{ph}}$ .

### Appendix B: Determining the critical phase space density $\mathcal{D}_B$

Estimates of  $\mathcal{D}_B(T_{\text{BKT}})$  for fermionic superfluids are provided in Refs. [16, 17], with values ranging from approximately 4.9 to 6.45. In comparison, the analogous systems in atomic Bose gases typically hover around 8 [6]. The lowest value,  $\mathcal{D}_B(T_{\text{BKT}}) = 4.9$ , which is the closest to the factor of 4 in the usual Nelson-Kosterlitz BKT relation, was reported to offer the best fit for the experimental results on Fermi gases [17]. In Ref. [18],  $\mathcal{D}_B(T_{\text{BKT}})$  was taken at fixed value of 4.9. Here we consider a broader range of interaction and thus include the loglog dependence, albeit very weak, of  $\mathcal{D}_B$  on  $a_{2D}$ , and take the data from experiment. To this end, we take the data of  $\tilde{g}$  from the Supplemental Materials of Ref. [17], and plot in Fig. 7. The data fits perfectly to Eq. (6) in the text. Also plotted in the figure is the function with the identification of potential radius [25] or pair size [33] with  $a_{2D}$ . The small difference between these two curves reveals that  $a_{2D}$  differs from either potential radius or pair size.

- 
- [1] N. D. Mermin and H. Wagner, Absence of ferromagnetism or antiferromagnetism in one- or two-dimensional isotropic Heisenberg models, *Phys. Rev. Lett.* **17**, 1133 (1966).  
[2] V. Berezinskii, Destruction of long-range order in one-dimensional and two-dimensional systems possessing a continuous symmetry group. II. Quantum systems, *Sov. Phys. JETP*

**34**, 610 (1972).

- [3] J. M. Kosterlitz and D. J. Thouless, Ordering, metastability and phase transitions in two-dimensional systems, *J. Phys. C* **6**, 1181 (1973).  
[4] Z. Hadzibabic, P. Krüger, M. Cheneau, B. Battelier, and J. Dalibard, Berezinskii-Kosterlitz-Thouless crossover in a trapped

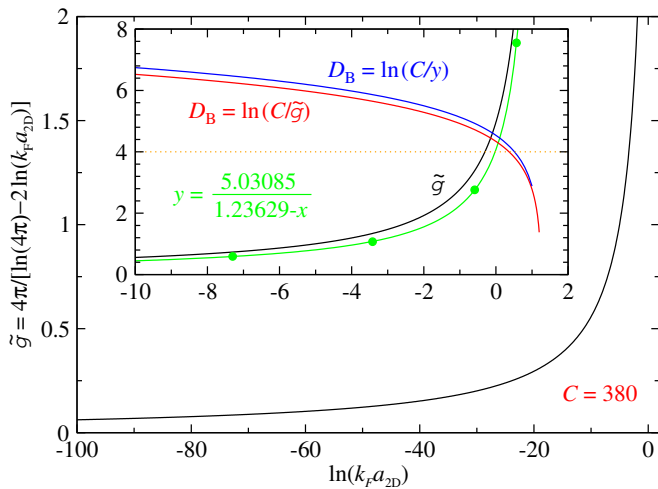


Figure 7.  $\tilde{g}$  as a function of  $\ln(k_F a_{2D})$  as given by the QMC result of Prokof'ev et al [25] (black solid line). Shown in the inset is the corresponding  $D_B$  (red line), along with the experimental data (green dots) and fit (green line) for  $\tilde{g}$  from Ref. [17]. The fit from experimental data yields a slightly larger  $D_B$  (blue line).

atomic gas, *Nature* **441**, 1118 (2006).

- [5] P. Cladé, C. Ryu, A. Ramanathan, K. Helmerson, and W. D. Phillips, Observation of a 2D Bose gas: From thermal to condensate to superfluid, *Phys. Rev. Lett.* **102**, 170401 (2009).
- [6] S. Tung, G. Lamporesi, D. Lobser, L. Xia, and E. A. Cornell, Observation of the presuperfluid regime in a two-dimensional Bose gas, *Phys. Rev. Lett.* **105**, 230408 (2010).
- [7] M. J. Kosterlitz, Kosterlitz-Thouless physics: a review of key issues, *Rep. Prog. Phys.* **79**, 26001 (2016).
- [8] V. M. Loktev, R. M. Quick, and S. G. Sharapov, Phase fluctuations and pseudogap phenomena, *Physics Reports* **349**, 1 (2001).
- [9] Q. J. Chen, Z. Q. Wang, R. Boyack, S. L. Yang, and K. Levin, When superconductivity crosses over: From BCS to BEC, *Rev. Mod. Phys.* **96**, 025002 (2024).
- [10] I. Hetel, T. R. Lemberger, and M. Randeria, Quantum critical behaviour in the superfluid density of strongly underdoped ultrathin copper oxide films, *Nature Physics* **3**, 700 (2007).
- [11] W. Zhao, Q. Wang, M. Liu, W. Zhang, Y. Wang, M. Chen, Y. Guo, K. He, X. Chen, Y. Wang, J. Wang, X. Xie, Q. Niu, L. Wang, X. Ma, J. K. Jain, M. Chan, and Q.-K. Xue, Evidence for berezinskii-kosterlitz-thouless transition in atomically flat two-dimensional pb superconducting films, *Solid State Communications* **165**, 59 (2013).
- [12] I. Božović, X. He, J. Wu, and A. T. Bollinger, Dependence of the critical temperature in overdoped copper oxides on superfluid density, *Nature* **536**, 309 (2016).
- [13] D. F. Agterberg, T. Shishidou, J. O'Halloran, P. M. R. Brydon, and M. Weinert, Resilient nodeless *d*-wave superconductivity in monolayer FeSe, *Phys. Rev. Lett.* **119**, 267001 (2017).
- [14] Y.-T. Hsu, A. Vaezi, M. H. Fischer, and E.-A. Kim, Topological superconductivity in monolayer transition metal dichalcogenides, *Nature Communications* **8**, 14985 (2017).
- [15] Y. Cao, V. Fatemi, S. Fang, K. Watanabe, T. Taniguchi, E. Kaxiras, and P. Jarillo-Herrero, Unconventional superconductivity in magic-angle graphene superlattices, *Nature* **556**, 43 (2018).
- [16] M. G. Ries, A. N. Wenz, G. Zürn, L. Bayha, I. Boettcher, D. Kedar, P. A. Murthy, M. Neidig, T. Lompe, and S. Jochim, Observation of pair condensation in the quasi-2D BEC-BCS crossover, *Phys. Rev. Lett.* **114**, 230401 (2015).
- [17] P. A. Murthy, I. Boettcher, L. Bayha, M. Holzmann, D. Kedar, M. Neidig, M. G. Ries, A. N. Wenz, G. Zürn, and S. Jochim, Observation of the Berezinskii-Kosterlitz-Thouless phase transition in an ultracold Fermi gas, *Phys. Rev. Lett.* **115**, 010401 (2015).
- [18] X. Y. Wang, Q. J. Chen, and K. Levin, Strong pairing in two dimensions: pseudogaps, domes, and other implications, *New Journal of Physics* **22**, 063050 (2020).
- [19] T. Shi, W. Zhang, and C. A. R. S. de Melo, Tighter upper bounds on the critical temperature of two-dimensional superfluids and superconductors from the bcs to the bose regime, *New Journal of Physics* **26**, 093001 (2024).
- [20] S. S. Botelho and C. A. R. S. de Melo, Vortex-antivortex lattice in ultracold fermionic gases, *Physical Review Letters* **96**, 040404 (2006).
- [21] M. Bauer, M. M. Parish, and T. Enss, Universal equation of state and pseudogap in the two-dimensional Fermi gas, *Phys. Rev. Lett.* **112**, 135302 (2014).
- [22] G. Bighin and L. Salasnich, Finite-temperature quantum fluctuations in two-dimensional Fermi superfluids, *Phys. Rev. B* **93**, 014519 (2016).
- [23] B. C. Mulkerin, L. He, P. Dyke, C. J. Vale, X.-J. Liu, and H. Hu, Superfluid density and critical velocity near the Berezinskii-Kosterlitz-Thouless transition in a two-dimensional strongly interacting Fermi gas, *Phys. Rev. A* **96**, 053608 (2017).
- [24] C.-T. Wu, B. M. Anderson, R. Boyack, and K. Levin, Quasi-condensation in two-dimensional Fermi gases, *Phys. Rev. Lett.* **115**, 240401 (2015).
- [25] N. Prokof'ev, O. Ruebenacker, and B. Svistunov, Critical point of a weakly interacting two-dimensional Bose gas, *Phys. Rev. Lett.* **87**, 270402 (2001).
- [26] Q. J. Chen, I. Kosztin, B. Jankó, and K. Levin, Pairing fluctuation theory of superconducting properties in underdoped to overdoped cuprates, *Phys. Rev. Lett.* **81**, 4708 (1998).
- [27] J. R. Schrieffer, *Theory of superconductivity*, 1st ed. (W.A. Benjamin Inc., New York, 1964).
- [28] L. P. Gor'kov and T. K. Melik-Barkhudarov, Contribution to the theory of superconductivity in an imperfect Fermi gas, *Sov. Phys. JETP* **13**, 1018 (1961), [*J. Exptl. Theoret. Phys. (USSR)* **40**, 1452-1458 (1961)].
- [29] H. Heiselberg, C. J. Pethick, H. Smith, and L. Viverit, Influence of induced interactions on the superfluid transition in dilute Fermi gases, *Phys. Rev. Lett.* **85**, 2418 (2000).
- [30] D.-H. Kim, P. Törmä, and J.-P. Martikainen, Induced interactions for ultracold Fermi gases in optical lattices, *Phys. Rev. Lett.* **102**, 245301 (2009).
- [31] Z.-Q. Yu, K. Huang, and L. Yin, Induced interaction in a Fermi gas with a BEC-BCS crossover, *Phys. Rev. A* **79**, 053636 (2009).
- [32] Q. J. Chen, Effect of the particle-hole channel on BCS-Bose-Einstein condensation crossover in atomic Fermi gases, *Scientific Reports* **6**, 25772 (2016).
- [33] D. S. Petrov, M. A. Baranov, and G. V. Shlyapnikov, Superfluid transition in quasi-two-dimensional Fermi gases, *Phys. Rev. A* **67**, 031601 (2003).
- [34] Q. J. Chen, I. Kosztin, B. Jankó, and K. Levin, Superconducting transitions from the pseudogap state: *d*-wave symmetry, lattice, and low-dimensional effects, *Phys. Rev. B* **59**, 7083 (1999).
- [35] Q. J. Chen, K. Levin, and I. Kosztin, Superconducting phase coherence in the presence of a pseudogap: Relation to specific heat, tunneling, and vortex core spectroscopies., *Phys. Rev. B* **63**, 184519 (2001).

- [36] Q. J. Chen, J. Stajic, and K. Levin, Applying BCS-BEC crossover theory to high temperature superconductors and ultracold atomic Fermi gases, *Low Temp. Phys.* **32**, 406 (2006), [*Fiz. Nizk. Temp.* **32**, 538-560 (2006)].
- [37] Q. J. Chen, J. Stajic, S. N. Tan, and K. Levin, BCS-BEC crossover: From high temperature superconductors to ultracold superfluids, *Phys. Rep.* **412**, 1 (2005).
- [38] J. Kinast, A. Turlapov, J. E. Thomas, Q. J. Chen, J. Stajic, and K. Levin, Heat capacity of a strongly interacting Fermi gas, *Science* **307**, 1296 (2005).
- [39] Q. J. Chen and K. Levin, Momentum resolved radio frequency spectroscopy in trapped Fermi gases, *Phys. Rev. Lett.* **102**, 190402 (2009).
- [40] Q. J. Chen and J. B. Wang, Pseudogap phenomena in ultracold atomic Fermi gases, *Front. Phys.* **9**, 539 (2014).
- [41] X. Li, S. Wang, X. Luo, Y.-Y. Zhou, K. Xie, H.-C. Shen, Y.-Z. Nie, Q. J. Chen, H. Hu, Y.-A. Chen, X.-C. Yao, and J.-W. Pan, Observation and quantification of the pseudogap in unitary Fermi gases, *Nature* **626**, 288 (2024).
- [42] L. P. Kadanoff and P. C. Martin, Theory of many-particle systems. ii. superconductivity, *Phys. Rev.* **124**, 670 (1961).
- [43] Q. J. Chen, *Generalization of BCS theory to short coherence length superconductors: A BCS-Bose-Einstein crossover scenario*, Ph.D. thesis, University of Chicago (2000), available as arXiv:1801.06266.
- [44] A. L. Fetter and J. D. Walecka, *Quantum theory of many-particle systems* (McGraw-Hill, 1971).
- [45] J. Levinsen and M. M. Parish, Strongly interacting two-dimensional Fermi gases, in *Annual Review of Cold Atoms and Molecules* (World Scientific, 2015) Chap. CHAPTER 1, pp. 1–75.
- [46] J. M. Kosterlitz and D. J. Thouless, Early work on defect driven phase transitions, *International Journal of Modern Physics B* **30**, 1630018 (2016).
- [47] N. Prokof'ev and B. Svistunov, Two-dimensional weakly interacting Bose gas in the fluctuation region, *Phys. Rev. A* **66**, 043608 (2002).
- [48] Note that the concrete value of  $\mathcal{D}_B$  will have a slight quantitative impact on  $T_{\text{BKT}}$  in the unitary regime. Such an impact becomes negligible in the BCS regime where both  $(n_s/m)$  and  $n_B/M_B$  decrease rapidly with  $T$  around  $T_{\text{BKT}}$  so that  $T_{\text{BKT}} \approx T_c^{\text{MF}}$ .
- [49] M. Randeria, J.-M. Duan, and L.-Y. Shieh, Superconductivity in a two-dimensional Fermi gas: Evolution from Cooper pairing to Bose condensation, *Phys. Rev. B* **41**, 327 (1990).
- [50] L. Gor'kov and T. Melik-Barkhudarov, Contribution to the theory of superfluidity in an imperfect Fermi gas, *Sov. Phys. JETP* **13**, 1018 (1961).
- [51] It should be noted that  $\mu = 0$  occurs at  $\ln(k_F a_{2D}) \approx -0.25$  and  $-0.175$  for level 1 and 2 averaging, respectively, as they are calculated with the self-consistent solutions of  $T_{\text{BKT}}$ .
- [52] L. Sobirey, N. Luick, M. Bohlen, H. Biss, H. Moritz, and T. Lompe, Observation of superfluidity in a strongly correlated two-dimensional Fermi gas, *Science* **372**, 844 (2021), <https://www.science.org/doi/pdf/10.1126/science.abc8793>.
- [53] Y.-Y. He, H. Shi, and S. W. Zhang, Precision many-body study of the Berezinskii-Kosterlitz-Thouless transition and temperature-dependent properties in the two-dimensional Fermi gas, *Phys. Rev. Lett.* **129**, 076403 (2022).
- [54] We note that, in Ref. [22], the expressions for the normal fluid densities  $n_{n,f}$  and  $n_{n,b}$  in their Eqs. (15-16) were wrong by a dimensionful factor  $1/m$ .
- [55] D. S. Petrov and G. V. Shlyapnikov, Interatomic collisions in a tightly confined Bose gas, *Phys. Rev. A* **64**, 012706 (2001).